Received: 3 July 2019 | Revised: 9 October 2019 | Accepted: 10 October 2019

DOI: 10.1111/gcb.14873

PRIMARY RESEARCH ARTICLE

Global Change Biology WILEY

Accurate forest projections require long-term wood decay experiments because plant trait effects change through time

Brad Oberle[1,2] | Marissa R. Lee[3] | Jonathan A. Myers[4] | Oyomoare L. Osazuwa-Peters[5] | Marko J. Spasojevic[6] | Maranda L. Walton[4] | Darcy F. Young[7] | Amy E. Zanne[7]

[1]Division of Natural Sciences, New College of Florida, Sarasota, FL, USA

[2]Center for Conservation and Sustainable Development, Missouri Botanical Garden, St. Louis, MO, USA

[3]Department of Plant and Microbial Biology, North Carolina State University, Raleigh, NC, USA

[4]Department of Biology, Washington University in St. Louis, St. Louis, MO, USA

[5]Division of Biostatistics, Washington University School of Medicine, St. Louis, MO, USA

[6]Department of Evolution, Ecology, and Organismal Biology, University of California Riverside, Riverside, CA, USA

[7]Department of Biological Sciences, The George Washington University, Washington, DC, USA

Correspondence
Brad Oberle, Division of Natural Sciences, New College of Florida, 5800 Bay Shore Rd., Sarasota, FL 34243, USA.
Email: boberle@ncf.edu

Funding information
Division of Environmental Biology, Grant/Award Number: 1302797 and 1557094

Abstract

Whether global change will drive changing forests from net carbon (C) sinks to sources relates to how quickly deadwood decomposes. Because complete wood mineralization takes years, most experiments focus on how traits, environments and decomposer communities interact as wood decay begins. Few experiments last long enough to test whether drivers change with decay rates through time, with unknown consequences for scaling short-term results up to long-term forest ecosystem projections. Using a 7 year experiment that captured complete mineralization among 21 temperate tree species, we demonstrate that trait effects fade with advancing decay. However, wood density and vessel diameter, which may influence permeability, control how decay rates change through time. Denser wood loses mass more slowly at first but more quickly with advancing decay, which resolves ambiguity about the after-life consequences of this key plant functional trait by demonstrating that its effect on decay depends on experiment duration and sampling frequency. Only long-term data and a time-varying model yielded accurate predictions of both mass loss in a concurrent experiment and naturally recruited deadwood structure in a 32-year-old forest plot. Given the importance of forests in the carbon cycle, and the pivotal role for wood decay, accurate ecosystem projections are critical and they require experiments that go beyond enumerating potential mechanisms by identifying the temporal scale for their effects.

KEYWORDS
carbon cycle, plant traits, temperate forest, temporal scale, wood decay, woody debris

1 | INTRODUCTION

Deadwood is a large above-ground carbon (C) pool that influences how forests respond to global change (Edburg et al., 2012; Pan et al., 2011). After woody tissues senesce, many of the same plant traits that promote tree longevity resist biological decay. Few organisms can rapidly degrade lignified secondary cell walls characteristic of woody tissues (Harmon et al., 1986; Weedon et al., 2009). Consequently, woody debris (WD) may have C residence times an order of magnitude longer than leaf litter and can remain in forests for years to decades (Pietsch et al., 2014). Due to slow decomposition, WD can delay C emissions following major forest disturbances (Edburg et al., 2012). For example, after a beetle outbreak decimated living trees, a western North American forest temporarily emitted less C because soil respiration fell more than the increase in deadwood respiration (Moore et al., 2013). However, in this forest and others affected by dieback, eventual carbon efflux from deadwood may exceed primary productivity, flipping the forests from C sinks to sources. Deadwood also influences other nutrient cycles, for instance as a temporary sink for N, with related impacts on

productivity and C uptake (Zimmerman et al., 1995). Since forests play such a major role in the terrestrial C cycle, predicting how carbon balance will respond to changing disturbance regimes requires identifying the factors that influence the full temporal trajectory of wood decay from senescence to complete mineralization.

Variation in wood decay rates reflects the combined influences of intrinsic and extrinsic drivers (Cornwell et al., 2009; Zanne et al., 2015). Wider stems from species with denser, more nutrient-limited wood tend to decompose more slowly (Hu et al., 2018; Weedon et al., 2009). Decay rates also depend on features of the surrounding environment, such that higher soil nutrient availability, temperature, and moisture tend to accelerate decay (Fravolini et al., 2016; Gora, Sayer, Turner, & Tanner, 2018). Ultimately, decay rates reflect activity of decomposing organisms, including fungi, bacteria, archaea, and animals, which interact with changing substrates, external environments, and one another (Van Der Wal, Ottosson, & De Boer, 2015).

Despite a growing list of candidate wood decay drivers, scaling up from experimental results to accurate forest ecosystem projections has proven considerably more challenging for several reasons. First, different mechanisms that drive decay can interact in complex ways. For example, in experimental wood decay microcosms, the effect of temperature depended on both fungus identity and substrate quality (Venugopal, Junninen, Edman, & Kouki, 2017). A second major challenge is identifying the spatial scale where important drivers and interactions emerge. Many experiments ignore environmental variability over small spatial scales, which can distort the relative explanatory power of, for instance, microclimate versus edaphic conditions (Bradford et al., 2014). Careful experiments and hierarchical models are beginning to resolve where certain drivers control decay (Bradford et al., 2017). However, a third remaining major challenge is to identify when these processes are most relevant. Scaling from short-term experiments to long-term processes requires extrapolating beyond the temporal domain of the data. Consequently, drivers that appear to be important when decay begins may have effects that ultimately change in magnitude or direction by the time most mass loss has occurred.

To illustrate how experimental timescale influences forest C projections, consider an experiment designed to test how variation in a tree functional trait drives deadwood residence times (Figure 1). In this example, the trait value controls how decay rates change compared to the negative exponential, or NegExp, decay model (central grey curve). The NegExp model assumes constant proportional mass loss as controlled by a single parameter. Because this model is applicable to experiments designed to sample mass loss only once, it is a common choice for representing decomposition despite known limitations for representing dynamic decay processes (Adair, Hobbie, & Hobbie, 2010). As the example demonstrates, sampling once and assuming NegExp decay can distort the relationship between trait values and decay. Because samples from the species with high trait values have lost relatively less mass at first, but more mass later on, the apparent relationship between trait values and residence time depends on experiment duration. Long-term decay data produce a trait effect in the correct direction but of reduced magnitude, intermediate-term data show no significant relationship, and short-term

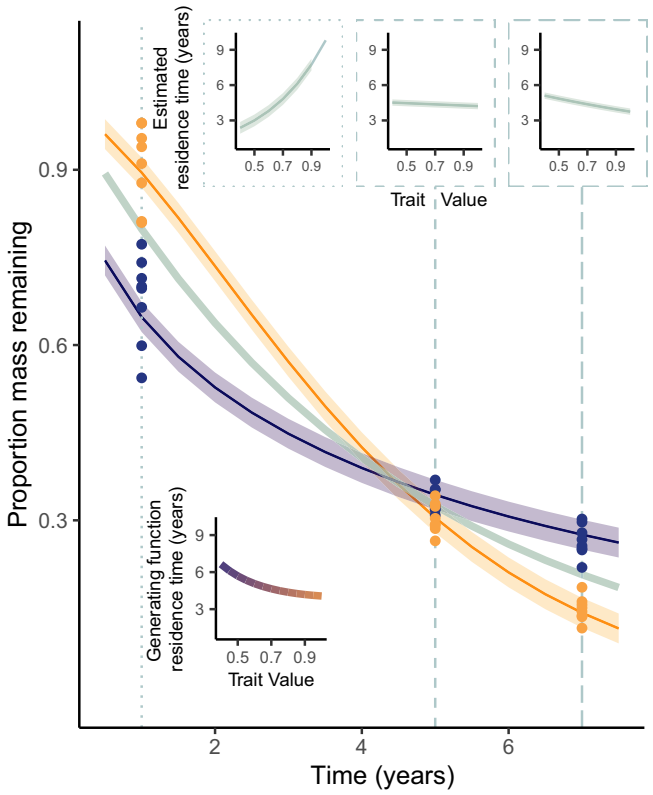

FIGURE 1 Hypothetical example illustrating how experimental timescale influences deadwood residence time estimates. Points represent mass loss from replicates of two tree species, one with high values of an important functional trait (light grey) and another with low values (dark grey). The generating function (lower left inset) is a hierarchical Weibull model (Equations 1 and 3) where the trait has a positive log-linear correlation with the value of the shape parameter (i.e. c Equation 1). The mass loss curves for both species intersect at time equal to the reciprocal of their common scale parameter (i.e. λ Equation 1). The curve from the associated NegExp model is illustrated in medium grey. Inset panels represent the inferred relationships between residence time and trait values at different sampling times (dashed vertical lines) [Colour figure can be viewed at wileyonlinelibrary.com]

data incorrectly imply that the trait strongly increases residence times. Any of these distorted relationships would lead to inaccurate representations of forest processes as an artefact of experimental timescale and associated misspecification of the underlying decay model. How long a decay experiment lasts and how frequently samples are collected may control what traits appear to be important, the directions of their effects, and associated projections of deadwood dynamics.

Here we tested how decay experiment duration and sampling frequency influenced the strength of candidate plant trait and environmental drivers, their roles in different functional forms for decay and the consequences for accurately predicting mass loss and deadwood structure. We integrated data from three complementary studies: a common-garden wood decay experiment involving 21 woody species decomposing for up to 7 years in two contrasting habitats, a concurrent experiment for validating mass loss projections, and

a WD inventory of naturally recruited deadwood in a 32-year-old forest dynamics plot at the same site. For the decay experiment involving all 21 species, we analysed mass loss using a new hierarchical Bayesian approach that interpolated between the widely used NegExp model and a time-varying Weibull model (Feng & Li, 2001). We evaluated the strength for 23 candidate drivers, including tree species wood chemistry and anatomy, as well as plot edaphic and microclimatic variables using different sampling schemes to test two specific hypotheses. First, because decay changes the wood substrate itself, we predicted that significant drivers would change with the duration and sampling frequency of experiment. Second, we predicted that long-term data analysed using a flexible time-varying model would more accurately project both mass loss and natural WD structure than models based on short-term data, single sampling points, or NegExp models.

2 | MATIERALS AND METHODS

2.1 | Site description

The experiments and WD inventory occurred at the Tyson Research Center, USA, at the northeastern edge of the Ozark ecoregion (38°31′N, 90°33′W) with a mean annual temperature of 13.5°C and mean annual precipitation of 957 mm. Local topography varies across highly eroded limestone bedrock with distinct ridge top and valley bottom habitats that differ in soil chemistry and plant communities (Spasojevic, Turner, & Myers, 2016; Spasojevic, Yablon, Oberle, & Myers, 2014).

2.2 | Wood decay experiment

Eight common-garden 'rot-plots' were situated in the adjacent ridge top and valley bottom sites in four watersheds. For each plot, we harvested tissue from 21 species widely spread across seed plant families, representing different growth forms (Table S1). We processed healthy stems into replicates approximately 22 cm in length and 5–9 cm in midpoint diameter with an average value of 6.93 ± 0.04 (*SE*) cm. Using a relatively narrow diameter allowed us to include wood from shrubs and lianas that seldom reach the typical size threshold for coarse WD, that is 10 cm in diameter (Harmon et al., 1986). For every replicate, we measured initial wet mass. We then estimated initial dry mass from the dry mass to wet mass ratio (DMWMR) of additional segments that we collected from each harvested stem and dried to constant mass at 103°C (Zanne et al., 2015). The first cohort was deployed in 2009 and included wood from 16 species. The second cohort was deployed in 2011 and included segments from five new species, as well as the validation experiment consisting of replicated segments from three species that were also included in the first cohort (Table S1).

We harvested replicates on four occasions. In 2010, 2012, and 2014, we harvested one replicate per species per rot plot per cohort using the protocol described in Zanne et al. (2015). Briefly, we randomly selected replicates in a given year and collected all wood or bark residue except fragments small enough to pass through a 0.5 cm^2 mesh. We carefully removed adhered soil, insects, and fruiting bodies and measured the final wet mass for each sample. We surface sterilized logs, allowed the sterilizing solution to evaporate, and used a sterilized drill bit to collect approximately 1 g of sawdust from both the top and the bottom of logs for other analyses. Following sawdust collection, we reweighed the wet mass of the drilled log and dried them at 103°C for 48 hr. We estimated the dry mass at harvest as the product of the final wet mass and the measured DMWMR of the drilled sample.

In 2014, a laboratory accident damaged samples after weighing final wet mass and collecting sawdust subsamples but before drying the drilled logs. For these samples, we calculated moisture content using a multiple imputation approach (See Moisture content imputation). At the end of the harvest in 2014, decay had progressed so far among certain species and sites that we anticipated complete mineralization prior to the final planned harvest. We collected those samples using the same general protocol but directly measured dry mass. Specifically, we collected samples using the same field protocol including screening through the 0.5 cm^2 mesh, removing insects, fruiting bodies, and adhered soil. We then dried samples at 103°C for 48 hr to directly measure final dry mass. We harvested and directly measured dry mass for every remaining replicate during the final harvest in 2016.

2.3 | Moisture content imputation

As described above, a laboratory accident during the 2014 harvest damaged 108 samples after measuring wet mass and collecting sawdust subsamples but before measuring the drilled log dry mass. To estimate the log DMWMR, we measured the DMWMR of 493 sawdust subsamples representing all 256 logs from the harvest. Specifically, we weighed the wet mass of the sawdust, dried them to 103°C and reweighed them to a precision of 0.1 mg. In cases where more than one independent sawdust subsample was collected, we took the mean DMWMR of every subsample taken from the same log. We estimated the drilled log DMWMR for the damaged subsamples by regressing the measured log DMWMR onto the sawdust DMWMR. To better meet the assumptions of the regression, we logit transformed both the predictor (sawdust) and response (log) DMWMRs. Measured log DMWMRs were highly correlated with sawdust DMWMRs (r = .85, Figure S1). We then imputed the missing log DMWMR values while estimating the regression parameters in a Bayesian context with vague priors (i.e. Normal (0,1,000)) on the intercept and slope coefficients using Markov–Chain Monte Carlo (MCMC) sampling as implemented in rjags 4.6 (Plummer, 2016) in R v 3.1.1 (R Core Team, 2017). After discarding the first 1,000 samples as burn-in, we drew 2,000 samples from the posterior distribution from three independent MCMC chains representing both regression coefficients and, at each iteration, calculated the missing value of DMWMR for damaged log samples. We checked for convergence by visually inspecting the trace plots and ensuring that the Brooks–Gelman–Rubin (Brooks & Gelman, 1998) statistic was <1.03. We

substituted the mean of the imputed DMWMR when calculating mass loss for those samples. For all other samples from this harvest, we used the directly measured DMWMR of the drilled logs.

2.4 | Candidate drivers

To represent intrinsic drivers of decay, we analysed the initial wood chemical and anatomical traits. For wood chemistry, we analysed the natural log of the C:N ratio, carbon fractions (i.e. Cellulose%, Hemicellulose%, and log(Lignin%)) and concentrations of elements associated with wood decay enzymes (i.e. Ca, log(P), and Mn; Zanne et al., 2015). Anatomical traits were wood density, conduit lumen diameter (Zanne et al., 2015), and conduit length (Oberle, Ogle, Zuluaga, Sweeney, & Zanne, 2016). We also measured the fraction of cross-sectional area represented by parenchyma and conduit walls based on microscopic analysis of radial sectors of fixed, stained cross sections from three branches per species following the same methodology as (Osazuwa-Peters, Wright, & Zanne, 2017).

To represent extrinsic drivers of decay, we analysed the microclimate and soils. We measured air temperature and relative humidity at 1 m above the soil surface, as well as soil temperature and moisture content at 10 cm below the surface every 10 min from June 2011 to June 2014 using Hobo weather stations (Zanne et al., 2015). Because some sensors failed during this interval, we quantified plot-level microclimatic variation as the mean deviation from simultaneous measurements at a reference station that collected data for all four variables throughout the entire measurement period. For soil chemistry, we collected 8 cores from a depth of 1 to 10 cm within the original footprint of the rot plot in July 2012 and measured N content, soil pH, Total Exchangeable Bases, Bray P, Ca, and Mn using standard methods (Spasojevic et al., 2016; Spasojevic et al., 2014). Finally, we used a smoothed digital elevation model to calculate the topographic moisture index at every site (Oberle et al., 2015).

2.5 | WD inventory

We characterized WD structure based on a 2012 deadwood inventory in a 4 ha section of the 20 ha Tyson Research Center Forest Dynamics plot (Spasojevic et al., 2014). This portion of the plot was established in 1981. Every stem >2 cm diameter at 1.4 m height was tagged, identified, measured, and mapped. In 1989, mortality was noted and new recruits were added. Between 2010 and 2012, the plot was resurveyed and expanded using standard techniques (Anderson-Teixeira, Davies, Bennett, Muller-Landau, & Wright, 2014).

The 2012 deadwood inventory analysed here included several measurements of tagged deadwood within the original 4 ha forest dynamics plot (Oberle et al., 2015). Briefly, we classified vertical position of WD as either 'standing' or 'down' depending on whether it was suspended unsupported above 2 m height or had broken and fallen to the ground respectively. Depending on vertical position, we measured deadwood dimensions in different ways. For standing deadwood, we measured diameter above the root collar and at 1.4 m above the ground using a diameter tape. For down deadwood we measured the horizontal diameter at the base of the log at the most distal point that was at least 7 cm wide using timber calipers. For comparison with the decay experiment, we only analysed WD wider than 7 cm diameter at its widest end. In addition to measuring deadwood dimensions, we identified decay class (DC), using a standard classification system based on a progressive series of external indicators (Harmon, Fasth, Woodall, & Sexton, 2013; Oberle et al., 2015). DC1 still has attached twigs, DC2 has no twigs but retains most of its bark, DC3 has lost most of its bark but has an intact bole, DC4 has developed large holes, and DC5 cannot maintain its original shape.

To estimate the values of environmental covariates at the locations of deadwood, we conducted spatial analyses of variation in soil-surface temperature. Specifically, we used a dataset of soil-surface temperatures generated by 199 shielded iButton (Maxim Integrated) temperature loggers systematically distributed across the site (Spasojevic et al., 2016). Loggers measured temperatures at 2 hr intervals from July 11, 2013 to July 11, 2014. Because methods differed from the common-garden plots, we *z*-transformed the iButton data and rescaled them to have the same mean and standard deviation as air temperatures recorded over the same interval by the reference weather station for the common-garden plots. We fit an exponential variogram to the mean temperature-distance relationship and kriged the fitted variogram to a set of points in a 5 × 5 m square grid over the WD survey area using the R package 'sp' (Pebesma & Bivand, 2005).

Besides features of deadwood that we directly measured in the 2012 survey, we determined tree species identity using retained tags from prior living tree surveys. Among 434 tagged pieces of WD > 7 cm in diameter, 261 matched 12 species from the decay experiment. To assess whether the tagged deadwood pool that we included in the inventory was representative of potential deadwood recruits, we made two comparisons. First, we compared the distribution of residence times estimated from the best-fit decay model (see Model implementation, simplification, and adequacy) to the distribution of residence times for the same set of species in the living tree pool in the 2010–2012 survey of the 4 ha plot. Second, we compared the tagged deadwood residence time distribution to the distribution of residence times estimated for stems that had been recorded as alive in 1989 but were not recorded as tagged living stems during the 2010–2012 inventory. Because drought-related defoliation made *Amelanchier arborea* difficult to identify as dead during the inventory and because it appeared as anomalously overrepresented in the deadwood survey, we excluded this species from all analyses of deadwood structure. We tested whether estimated residence times differed between the set of tagged stems recovered in the deadwood inventory and the pool of stems missing from the 1989 inventory using logistic regression, with inventory as a binary response and estimated residence time as the predictor using the function 'glm' in r package 'stats' (R Core Team, 2017).

2.6 | Model structure

To represent decay in the experiment, we assumed that the proportion of mass remaining (M) for every replicate $i = 1 \ldots I$ with increasing time, t, since deployment for $j = 1 \ldots n$ species and $k = 1 \ldots m$ plots is defined by the Weibull function (Feng & Li, 2001):

$$M(t)_{ijk} = 1 - e^{-(\lambda_{jk} t_i)^{c_{jk}}}, \quad (1)$$

where λ is the scale parameter and c is the shape parameter. If the value of the shape parameter is >1, mass loss accelerates through time, which reduces residence times relative to the NegExp decay. If the value of the shape parameter is <1, mass loss decelerates through time, which increases residence times. Fixing the shape parameter at 1 yields the NegExp model.

$$M(t)_{ijk} = 1 - e^{-(\lambda_{jk} t_i)}. \quad (2)$$

To estimate the parameters of the Weibull function from observed data, we employed a generalized Weibull regression approach using a double log link function and normally distributed measurement-level error on the transformed scale (Oberle et al., 2016). Under this approach, the parameters of the Weibull decay function, λ_{jk}, c_{jk}, may vary with intrinsic features of wood and extrinsic features of the environment. Specifically, we treated λ_{jk} and c_{jk} as stochastic variables that depend in turn on hyperparameters in a multilevel regression framework:

$$\lambda_{jk} \sim \text{LogNormal}\left(\alpha_\lambda + \boldsymbol{W}\boldsymbol{g}_\lambda + \boldsymbol{X}\boldsymbol{h}_\lambda, \tau_\lambda\right), \quad (3)$$

where α_λ is the intercept for the scale parameter, $\boldsymbol{W}$ is a $I \times n$ matrix of species-level trait covariates and $\boldsymbol{g}_\lambda$ is a vector of n species trait effects, $\boldsymbol{X}$ is a $I \times m$ matrix of plot-level environmental covariates and $\boldsymbol{h}_\lambda$ is a vector of m environment effects, and τ_λ is the precision (inverse variance) for the scale parameter. An equivalent expression applies to a multilevel regression for the shape parameter, c_{jk}. The log-normal likelihood reflects the constraint that both λ_{jk} and c_{jk} must be positive. For NegExp decay, we fixed c to one and used the canonical log-link function with normally distributed measurement-level error (Oberle et al., 2016).

To determine which drivers predict variation in decay parameters we used a latent binary indicator variable approach (O'Hara & Sillanpää, 2009). Specifically, each element in the vector of $n + m$ multilevel regression coefficients (i.e. $\boldsymbol{g}_\lambda$ and $\boldsymbol{h}_\lambda$ in Equation 2) is represented as the product of a binary indicator variable, $I_{\lambda,j,k}$, and a latent regression coefficient, $\beta_{\lambda,j,k}$

$$\boldsymbol{g}_{\lambda,j,k} = I_{\lambda,j,k}\beta_{\lambda,j,k}. \quad (4)$$

When an indicator variable takes a value of 1, the corresponding covariate is included in the model. The probability that an indicator takes a value of 1 is treated as stochastic:

$$I_{\lambda,j,k} \sim \text{Bernoulli}\left(p_\lambda\right), \quad (5)$$

where p_λ is the probability of covariate inclusion as estimated by the data.

2.7 | Model implementation, simplification, and adequacy

We fit the decay model (Equations 1–5) in a Bayesian context using rjags v 4.6 using vague priors with broad distributions. For the residual measurement-level errors, we placed a broad uniform (0,10) prior on the residual standard deviation. We used the same prior for the error standard deviation in the lognormal hyperparameter regressions for the effects of species traits and environmental covariates (i.e. the square root of the reciprocal of τ_λ Equation 3). For the intercepts of the hyperparameter regressions (i.e. α_λ Equation 3), we used vague Normal (0,100) priors. As priors for the latent hyperparameter regression coefficients (i.e. $\beta_{\lambda,j,k}$ Equation 4), we used vague Normal (0,100) priors. Finally, for the prior on the proportion of important covariates, (i.e. p_λ Equation 5) we used a vague Beta (0.5,0.5) distribution which is symmetric around a minimum of 0.5.

We sampled from the posterior distributions using three independent MCMC chains with an adaptive burn-in phase of 10^4 iterations followed by 5×10^6 iterations, saving only every 50th sample. After quantifying the effective sample size, we extended chains, added additional chains, or adjusted the thinning interval until effective sample size numbers for all sampled quantities exceeded 1,000. We checked for convergence by visually inspecting the trace plots for the parameters and ensuring that the Brooks–Gelman–Rubin statistic was <1.03.

Simultaneously estimating multilevel regressions for Weibull shape and scale parameters using the same candidate predictors complicated sampling. To speed convergence for the full Weibull hyperparameter regression (Equations 1, 3–5), we sampled from a model with a simple normal (0,100) prior on the intercept for the scale parameter (e.g. α_λ Equation 3) while estimating the full parameter effects for the shape parameter and vice versa. After running consecutive, complementary models with hyperparameter regressions for shape and then scale parameters respectively, we included all covariates with 95% CI intervals that excluded 0 in our simplified models.

Following model simplification, we assessed the adequacy of alternative model specifications for different datasets. After analysing the full model, we reduced the set of predictors to those with 95% CIs that excluded 0 during simplification and substituted the binary latent indicator variable structure (i.e. Equation 4) for independent, vague normal (0,100) priors over each hyperparameter in the reduced vector of coefficients. We fit the models using the same approach described in model simplification but reduced the initial sampling phase to 5×10^5 iterations and the thinning interval to 10. After checking convergence, we drew an additional 2×10^5 samples for estimating the deviance information criterion (DIC, Spiegelhalter, Best, Carlin, & Van Der Linde, 2002). DIC is an analog for the more widely used Akaike information criterion (AIC, Akaike, 1973) that accommodates multilevel models where the number of parameters is estimated from the data. We selected the model with the lowest DIC as the most adequate model and report the mean of the posterior distribution and the limits of the 95%

CI for parameters of interest. For datasets including only the first or the fifth year of mass loss data, the Weibull model is not identifiable. For these subsets of the data, we compared the NegExp decay models.

To compare the predictive accuracy of different models against the validation dataset, we used two criteria. First, we re-expressed Equation (3) as

$$E\left(\lambda_{jk}\right)=e^{\alpha_\lambda+\mathbf{W}\mathbf{g}_\lambda+\mathbf{X}\mathbf{h}_\lambda+\frac{\sigma_\lambda^2}{2}}, \tag{6}$$

where the final term is the standard variance correction factor for lognormal regression. We used an equivalent expression for calculating the expected value of the shape parameter for Weibull decay. We substituted the expected parameter values into the expression for mass loss (Equations 1 or 2). From these, we calculated the root mean square deviation (RMSD), which decreases with increasing accuracy (Piñeiro, Perelman, Guerschman, & Paruelo, 2008). Secondly, we quantified accuracy by regressing observed mass loss onto predicted mass loss and tested the null hypotheses that unbiased predictions have an intercept of zero and a slope of one using ordinary least squares regression using function "lm" in R package "stats".

Because deadwood in the survey had naturally recruited at an unknown time, we calculated residence times for each piece of deadwood using trait and environmental covariates for different models. Under the Weibull decay function, the residence time $E(t)_{jk}$ is given by:

$$E(t)_{jk}=\frac{1}{\lambda_{jk}}\Gamma\left(1+\frac{1}{c_{jk}}\right), \tag{7}$$

where Γ is the gamma function (Feng & Li, 2001). Under NegExp decay, this expression simplifies to the reciprocal of λ_{jk}. We evaluated the effect of residence time on WD vertical position with standard logistic regressions with a two-sided hypothesis test as estimated using function 'glm' in R package 'stats' (R Core Team, 2017). We evaluated whether estimated residence times predict variation in WD DC as a proportional odds logistic regression with a two-sided hypothesis test using the 'polr' function in R package 'MASS' (Ripley, Venables, Bates, Hornik, & Firth, 2015). We compared models based on AIC with the goal of assessing whether the time varying model provided a more adequate prediction of naturally recruited deadwood structure than alternative models informed by fewer sampling points or the NegExp model.

2.8 | Parameter interpretation

To represent the relative importance of parameters in simplified models, we used three approaches. First, we calculated standardized effect sizes by dividing the magnitude of the regression coefficients by the standard deviation of the associated covariates. Because the response variables represent decay function parameters, which can be difficult to interpret with respect to mass loss, we also calculated average predictive comparisons (Oberle, Ogle, Zanne, & Woodall, 2018). This second approach compares the difference (Δ) in the response of interest (y) with a specified change (ξ) in a predictor variable of interest (x) as:

$$\Delta\left(\xi,\mathbf{t},x,\mathbf{X}\right)=\frac{\sum_{r=1}^{n}\left(E\left(y|x_r+\xi,\boldsymbol{\theta},\mathbf{X}_r\right)-E\left(y|x_r,\boldsymbol{\theta},\mathbf{X}_r\right)\right)}{n}, \tag{8}$$

where $\boldsymbol{\theta}$ represents the vector of other parameters $\mathbf{X}_r$ represents a matrix of residual covariates held at their means. Here the response of interest is the residence time estimated by the generalized regression (i.e. Equations (6) and (7). To represent uncertainty in average predictive comparisons, we estimated the 95% CI for each comparison based on 1,000 samples from the posterior distributions for the associated parameters (i.e. Equation 3).

Finally, we calculated the marginal effects of significant predictor effects for simplified models for all subsets of the data. For each significant predictor and simplified model, we randomly sampled 150 sets of parameter estimates from the converged MCMC chains. We substituted the parameter estimates into the generalized regression equation (i.e. Equations 6 and 7) to calculate the expected residence time for marginal differences in each predictor with all others held constant at their means. This approach illustrates the magnitude, direction, and uncertainty in the effect of each predictor on residence times.

3 | RESULTS

3.1 | Wood decay experiment

Experimental duration (i.e. 1e vs. 5 years of mass loss) and sampling frequency (i.e. once vs. three to four times) strongly influenced which candidate drivers influenced decay, the strength of their effects, and how they influenced the shape of the decay function. The common garden experiment involved 630 unique replicates and captured nearly complete mass loss for all species and sites. When the final replicates were harvested 5.7 years (±0.01 *SE*) after deployment, samples had lost 72.9% (±1.58 *SE*) of their initial mass. Among the 12 wood trait and 11 environmental candidate drivers (Figure 2; Table S2), the portions that was important for decay (i.e. p_λ in Equation 5) was highest when analysing only the first year of mass loss (year 1 NegExp, p_λ = 0.421, 95% CI = [0.225, 0.633]) and lowest when analysing only the fifth year of mass loss (year 5 NegExp, p_λ = 0.284, 95% CI = [0.091, 0.511]). After just 1 year, wood carbon fractions, branch density, and the proportion of parenchyma were associated with significantly slower decay rates while wood phosphorous was associated with significantly faster decay rates (Figure 2). Only log (lignin%) remained important after 5 years (Figure 2).

Analysing every sampling point in the time series identified many of the same predictors, but supported different effect magnitudes and functional relationships. Assuming NegExp decay, the proportion and identity of important predictors resembled those estimated after only 1 year (year 1–7 NegExp, p_λ = 0.410, 95% CI = [0.216, 0.622]). However, wood hemicellulose was not significant, while

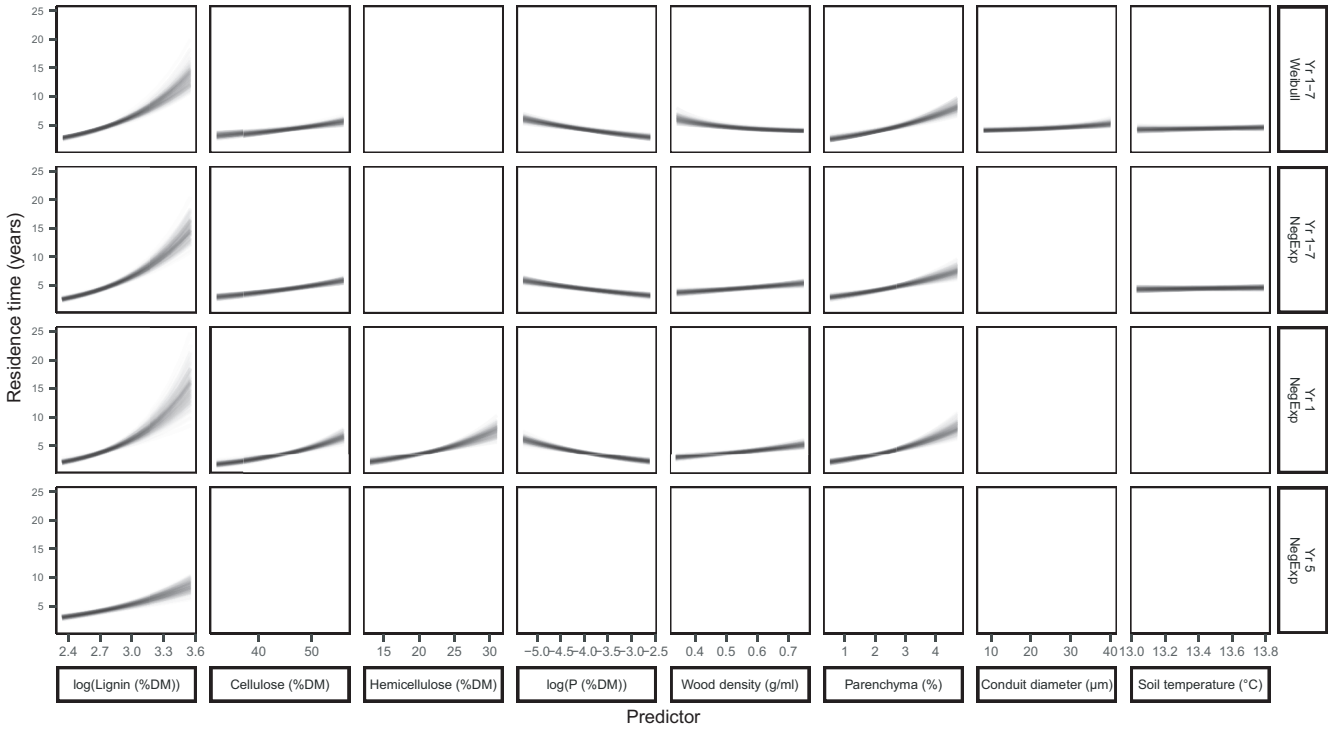

FIGURE 2 Tree species trait and environment predictors of wood decay vary with experimental timescale and decay function. The effects of each predictor on estimated residence times were estimated from the generalized regression (Equations 6 and 7) as marginal effects with other predictors held constant at their means. Curve overlays illustrate uncertainty using 150 sets of relevant parameters drawn from converged Markov–Chain Monte Carlo chains. Empty cells correspond to coefficients that had 95% credible intervals including 0 for a given temporal sampling scheme and functional form of decay

plot soil temperature slightly slowed decay (Figure 2). Compared to NegExp decay, a simplified Weibull decay model was much more adequate (year 1–7 NegExp DIC = −949.4; year 1–7 Weibull DIC = −990.4). Many of the same candidate decay drivers were associated with variation in the scale parameter of the Weibull distribution, which is functionally related to the scale parameter of the NegExp model. However, both initial wood density and xylem conduit diameter predicted variation in the Weibull shape parameter which controls how decay rates change through time. Wood density was associated with slow initial decay that accelerated relative to constant proportional mass while xylem conduit diameter had the opposite effect.

Differences in the direction and magnitudes of predictor effects between different sampling schemes translated to very different projections for deadwood residence times. Wood density exhibited a timescale dependent effect that changed from accelerating to slowing decay depending on the duration and model (Figure 2). Analysing the whole time series using the time-varying Weibull model resulted in denser wood having shorter residence times, while NegExp models implied that this trait had the opposite effect, with denser wood resulting in longer residence times. Differences in effect magnitudes for other wood traits translated to dramatically different projections of ecosystem dynamics (Figure 3). Lignin was the only trait that significantly influenced mass loss for every temporal sampling scheme and model. Based on the first year of decay, a species with modestly

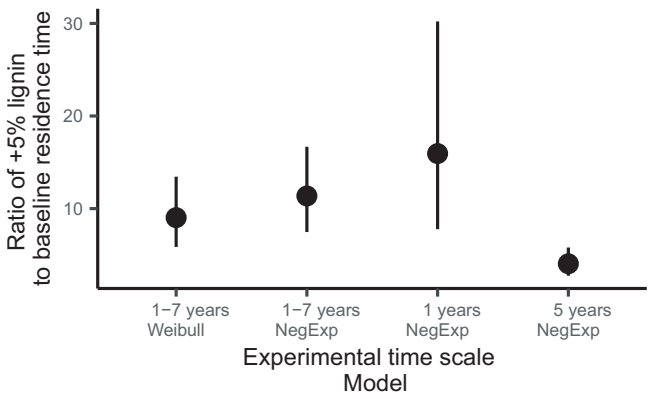

FIGURE 3 Experimental timescale influences how increased log (lignin%) increases deadwood residence time. All values are expressed as a ratio of residence times for a hypothetical species with 5% more lignin compared to the average species in the analysis. Points represent means of average predictive comparisons and whiskers representing 95% credible intervals

more lignin (5%) had projected residence times more than an order of magnitude longer, while estimating the impact of the same trait difference after 5 years projected to an increase in residence times by only a factor of four. Short-term data also yielded much more uncertain projections for the effect of increased lignin content on deadwood residence times.

3.2 | Validation experiment

For 72 additional replicates representing a subset of three species decaying at the same sites over 5 years, long-term data generated more accurate predictions of observed mass loss. Original and validation mass loss values for the same species, plots, and durations were weakly correlated (R^2 = .366) and were lower during the validation experiment. Model-based projections performed better but varied in accuracy depending on experimental timescale (Figure 4). A model parameterized by just the first year of decay data resulted in the least accurate predictions (RMSD = 0.217), although the overall relationship was unbiased (validation linear regression, R^2 = .498; intercept t [H_0 = 0] = −1.324, p = .19; slope t [H_0 = 1] = −0.785, p = .218). In comparison, a model parameterized with just the fifth year of decay data was more accurate (RMSD = 0.174), but marginally biased towards lower mass loss values (validation linear regression, R^2 = .689; intercept = −0.077, df = 2, t [H_0 = 0] = −1.988, p = .051; slope t [H_0 = 1] = −0.560, p = .289). Models parameterized using all of the decay data produced the most accurate predictions (year 1–7 NegExp RMSD = 0.161, year 1–7 Weibull RMSD = 0.163) and neither exhibited bias (year 1–7 NegExp, validation linear regression, R^2 = .664; intercept t [H_0 = 0] = −0.732, p = .467; slope t [H_0 = 1] = −0.845, p = .200; year 1–7 Weibull, validation linear regression, R^2 = .666; intercept t [H_0 = 0] = −0.540, p = .591; slope t [H_0 = 1] = −1.269, p = .104.

3.3 | WD inventory

Across a 4 ha, 32-year-old forest dynamics plot at the same site, estimates of residence time based on the full time series and Weibull decay accurately predicted naturally recruited deadwood structure. At the time of inventory, 261 tagged dead stems matched species from the decay experiment. Of these, 98 were standing unsupported above 2 m and intermediate DC were most common (DC 1 = 51, DC 2 = 73, DC 3 = 106, DC 4 = 24, DC 5 = 7). The ratio of standing to down deadwood among tagged stems was about 50% higher than the ratio of all standing to down deadwood among all stems greater than 7 cm in the inventory. Similarly, the average DC among tagged dead stems was 2.48 ± 0.06 (*SE*), which was slightly lower than the average DC among all stems greater than 7 cm diameter at the base (3.08 ± 0.03 *SE*). While the tagged dead stems tended to be relatively intact compared to deadwood overall, the distribution of residence time estimates in the deadwood pool was similar to that of living trees (Figure S2). Furthermore, estimated residence time was not a significant predictor for whether or a piece of deadwood was recovered with a tag from the pool of potential recruits that had gone missing from the plot since the previous inventory (Logistic Regression, n = 1,410, Weibull Residence effect, p = .1).

The most adequate model for deadwood position among naturally recruited tagged deadwood included both stem diameter and hierarchical Weibull residence times (Table S2). Controlling for the effect of stem

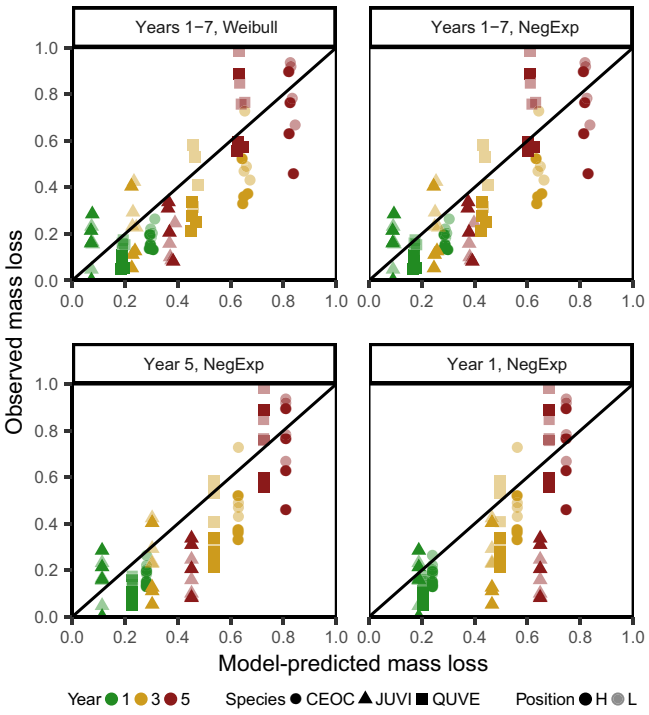

FIGURE 4 Timescale and decay function influence the accuracy of mass loss projections in a validation experiment. Species codes reflect the first two characters of the genus and species names (Table S1) and position denotes samples from plots on ridges (H) versus valleys (L) [Colour figure can be viewed at wileyonlinelibrary.com]

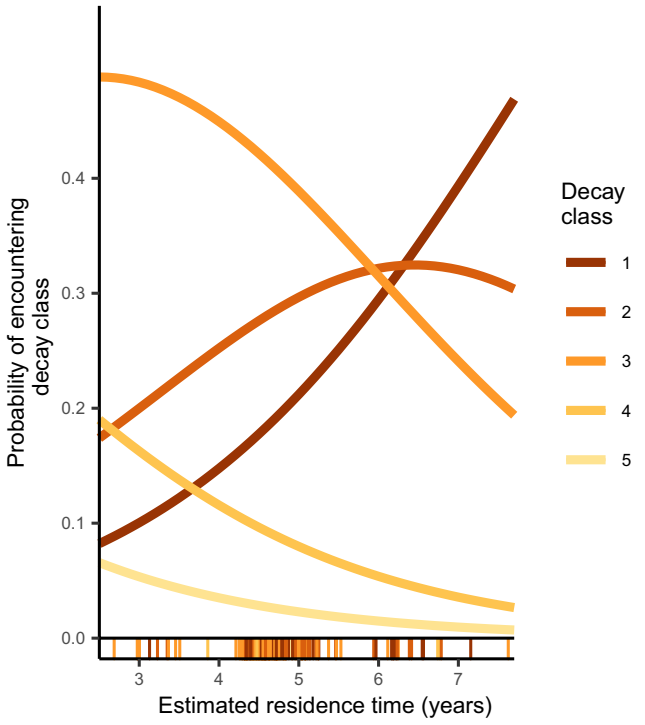

FIGURE 5 Naturally recruited woody debris (WD) with longer estimated residence time occurs in less advanced decay classes. Curves represent the marginal effect of residence times based on a Weibull model of wood decay for a hypothetical WD piece of average stem diameter [Colour figure can be viewed at wileyonlinelibrary.com]

diameter, WD from species and environments with longer projected residence times were marginally more likely to occur as standing (Figure S3, Logistic Regression, n = 261, diameter effect = 0.051, z = 3.56, p < .001, residence time effect = 0.397, z = 1.92, p = .055). Similarly, wider WD was more likely to occur in less advanced DCs, as was WD with longer projected residence times (Table S3; Figure 5, Proportional Odds Logistic Regression, n = 261, diameter effect = −0.0295, t = −2.306, p = .009, residence time effect = −0.393, t = −2.20, p = .012).

4 | DISCUSSION

As climate change stresses trees, forest carbon balance hinges on how quickly deadwood decomposes. Initial wood decay rates vary widely among tree species and sites, with short-term experiments emphasizing different roles for intrinsic and extrinsic drivers that can depend on spatial scale (Bradford et al., 2014; Weedon et al., 2009; Zanne et al., 2015). However, scaling from experiments to ecosystems also requires testing whether mechanisms that prevail when wood decay begins have the same influence as wood gradually mineralizes. Our results demonstrate how experimental timescale can distort mechanistic representations of decay in widely used empirical models with major consequences for projecting forest responses to disturbance.

4.1 | Trait effects depend on temporal scale

Consistent with our first hypothesis, based on the gradual changes in woody substrates during decay, the effects of trait and environmental drivers changed with timescale. As experiment duration increased, driver effects weakened and produced radically different relationships between traits and residence times. Fading effects of species traits has also been observed during long-term leaf litter decay (Moore, Trofymow, Prescott, & Titus, 2017). In a year-long experiment that captured complete mineralization of Mediterranean leaf litters, differences in intact leaf polyphenol content strongly influenced initial mineralization rates, but effect sizes decreased with increasing mass loss (García-Palacios, Shaw, Wall, & Hättenschwiler, 2016). Initial trait effects, like the traits themselves, may become less distinct as decomposers homogenize senesced plant tissues (Witkamp, 1966). While certain litter traits may have legacy or indirect effects mediated by distinct patterns of decomposer community assembly (Fukami et al., 2010), experiments that examine only the initial stage of wood decay may exaggerate trait effects that prevail early on but diminish with advancing decay.

Not only did timescale change the effects of drivers, it also changed their functional roles. Initial wood density provides an important example. Wood density is a key plant functional trait with an ambiguous effect on decay (Pietsch et al., 2014). A recent global meta-analysis found that denser wood decayed more quickly (Hu et al., 2018) in contrast to specific experiments that have either demonstrated slower decay for denser wood (Hérault et al., 2010) or no wood density effect (Freschet, Weedon, Aerts, van Hal, & Cornelissen, 2012; Kahl et al., 2017; Weedon et al., 2009). Our results can resolve these discrepancies by demonstrating that wood density may not control decay rates per se, but rather how decay rates change through time (i.e. Figure 1). Because the wood density effect depended on experimental timescale, we would expect that studies that involve more cumulative mass loss are more likely to recover a positive density-decay correlation than studies which are much shorter. Because wood density governs so many aspects of tree growth, competition, stress tolerance, and carbon storage (Cornwell et al., 2009), resolving how it relates to decay is essential for accurate forest carbon modelling and will require experiments that analyse mass loss at multiple time points for contrasting species using more flexible decay models than the standard NegExp.

Wood density was not the only trait with a timescale-dependent effect. Vessel diameter also changed the shape of the decay curve but in the opposite direction. Together, vessel diameter and wood density may mediate biological feedbacks related to substrate permeability and decomposability. Denser wood with narrow vessels may have more inaccessible internal cavities that breakdown faster as decay increases microbial access, microscale surface area to volume, and defensive compound leaching (Cornwell et al., 2009; Harmon et al., 1986). This interpretation is consistent with the results of an experiment analysing monthly mass loss across almost 3 years of decay among 32 tree species in Borneo, where species with initially more permeable wood decayed faster than exponential while those with dense wood decomposed more slowly (Mori et al., 2014). Further experiments could explore underlying mechanisms by connecting changes in bulk wood properties with variation in microbial community assembly and function.

Compared to wood traits, candidate environmental drivers had weak or unexpected effects. Differences in soil chemistry and temperature between habitats strongly influence living tree community structure (Spasojevic et al., 2014), but only soil temperature weakly slowed decay in the full-time series. This unexpected result conflicts with expectations based on temperature dependence of enzyme kinetics, but is consistent with at least one other experiment which found that leaves in warmer sites decayed more slowly (Fravolini et al., 2016). It is possible that slightly slower decay for species in warmer sites reflects physical hardening of exposed wood as has been noted at this site (Oberle et al., 2014). Furthermore, the temperature gradients present at our site (<1°C) are much smaller than gradients observed in studies that examine broad biogeographic gradients in wood decay (Adair et al., 2008; Bradford et al., 2017). Nevertheless, variation in initial wood traits more strongly influenced wood decay than environmental variability, which is consistent with global patterns (Hu et al., 2018; Weedon et al., 2009).

4.2 | Long-term data, frequent sampling, and flexible models make more accurate ecosystem projections

Consistent with our second hypothesis, accounting for dynamic wood trait effects generated more accurate predictions. In the

validation experiment, the least accurate predictions were based on short-term results, when trait effects were strongest. More accurate predictions came from a much weaker relationship between initial log(lignin%) and long-term decay, although this relationship was slightly biased towards lower mass loss values. Overall, models based on more traits and longer time series were more accurate and unbiased, predicting as much as 66% of the observed variation in mass loss. For applications that require more accurate predictions of long-term decay dynamics, particularly in systems where wood decays slowly or provides particularly valuable services, models informed by experiments with repeated harvests and multiple candidate drivers may provide the needed accuracy.

The ultimate goal of scaling up from experiments to ecosystem dynamics requires assessing model predictions in natural systems. Our results provide the first direct connection between experimental wood decay and naturally recruited deadwood structure across a heterogeneous landscape. We note that many factors could influence the probability of encountering a dead stem with a tag, including varying tree mortality, trait-based tag shedding, and overall decay rates obscuring the presence of stems. Even so, we found that the distribution of deadwood residence times in the tagged deadwood pool was very similar to the distribution of residence times for corresponding species in the living wood pool. Furthermore, estimated residence time did not predict whether a tag that had gone missing from a living tree was recovered on WD. Both results suggest that the tagged deadwood pool is unbiased with respect to decay rates even though tagged deadwood tended to be relatively intact. Within this broadly representative subset of deadwood, we compared how accurately different temporal sampling schemes and decay models predicted key aspects of deadwood structure. We found that long-term data with timescale-dependent effects were necessary for accurate predictions. Dead trees with quickly decomposing wood, as determined using a time-varying Weibull model, were more somewhat more likely to be broken, which is consistent with an analysis of standing dead tree fall across the eastern United States, where wood decay resistance was among the most important predictors of snag half-life (Oberle et al., 2018). While a model with Weibull residence times only marginally outperformed the null model for deadwood position, Weibull residence times provided a much more accurate projection of WD DC than residence times derived from any other model. Short-term data and simple models failed to predict variation in tagged deadwood DC, with major implications for scaling up experimental results because decay classification is the basis for estimating deadwood C content in the US National Forest Inventory (Harmon, Woodall, Fasth, & Sexton, 2008). While long-term data and a flexible model were necessary for accurate predictions, other factors can contribute to variation in deadwood structure observed at a particular point in time. For example, it is possible that we recovered relatively intact wood that had longer estimated residence times because the same traits that control decay also control tree mortality. To limit this possibility, we excluded observations of *Amelanchier arborea*, a species with relatively slowly decomposing wood, because it was severely impacted by drought and difficult to be classified as dead. In the future, resolving this ambiguity will require more comprehensive forest C models that include trait-based mortality and wood decay.

By finding that timescale influences how wood traits influence decay, our study emphasizes how short-term studies and correspondingly simple empirical models can misrepresent long-term ecosystem dynamics. In a recent review of litter decay experiments in the boreal zone, very few (11%) lasted long enough to capture major changes in decay rates that emerged after 12 years (Moore et al., 2017). While short-term data may be sufficient for testing hypotheses about factors that influence initial decay rate variation, they may rush to conclusions about transient mechanisms. More importantly, analyses that cannot accommodate dynamic decay rates may distort the roles for underlying drivers and produce radically different ecosystem projections. With global change driving forest dieback, understanding what controls wood decay has never been more urgent. When it comes to accurately representing wood decay in earth system models, our results show that long-term experiments are worth the wait.

ACKNOWLEDGEMENTS

We thank the National Science Foundation (DEB 1302797 to AEZ and DEB 1557094 to JAM and MJS), the International Center for Energy, Environment and Sustainability at Washington University in St. Louis, the Smithsonian Institution Center for Tropical Forest Science-Forest Global Earth Observatory, the Office of the Provost of New College of Florida, and Tyson Research Center for supporting our work. We thank the Tyson Research Center staff for providing logistical support, the more than 100 students and researchers that have contributed to data collection, and C. Hampe and V. Sork for establishing the plot and sharing tag information. K. Dunham, E. Hernandez, and A. Milo contributed to decay data and WD inventory collection. W. Cornwell gave helpful comments on an early draft. Two anonymous reviewers provided insightful comments that substantially improved the manuscript.

CONFLICT OF INTEREST

The authors declare no conflicts of interest.

ORCID

Brad Oberle https://orcid.org/0000-0002-4227-3352

REFERENCES

Adair, E. C., Hobbie, S. E., & Hobbie, R. K. (2010). Single-pool exponential decomposition models: Potential pitfalls in their use in ecological studies. *Ecology*, *91*(4), 1225–1236. https://doi.org/10.1890/09-0430.1. Retrieved from http://www.ncbi.nlm.nih.gov/pubmed/20462136

Adair, E. C., Parton, W. J., Del grosso, S. J., Silver, W. L., Harmon, M. E., Hall, S. A., … Hart, S. C. (2008). Simple three-pool model accurately describes patterns of long-term litter decomposition in diverse

climates. *Global Change Biology*, *14*(11), 2636–2660. https://doi.org/10.1111/j.1365-2486.2008.01674.x

Akaike, H. (1973). Information theory and an extension of the maximum likelihood principle. In B. N. Petran & F. Csaki (Eds.), *International symposium on information theory* (pp. 267–281). Budapest, Hungary: Akademiai Kiadi.

Anderson-teixeira, K. J., Davies, S. J., Bennett, A. M. Y. C., Muller-landau, H. C., & Wright, S. J. (2014). CTFS-ForestGEO : A worldwide network monitoring forests in an era of global change. *Global Change Biology*, *21*, 528–549. https://doi.org/10.1111/gcb.12712

Bradford, M. A., Veen, G. F., Bonis, A., Bradford, E. M., Classen, A. T., Cornelissen, J. H. C., … van der Putten, W. H. (2017). A test of the hierarchical model of litter decomposition. *Nature Ecology and Evolution*, *1*(12), 1836–1845. https://doi.org/10.1038/s41559-017-0367-4

Bradford, M. A., Warren II, R. J., Baldrian, P., Crowther, T. W., Maynard, D. S., Oldfield, E. E., … King, J. R. (2014). Climate fails to predict wood decomposition at regional scales. *Nature Climate Change*, *4*(7), 625–630. https://doi.org/10.1038/nclimate2251

Brooks, S. P., & Gelman, A. (1998). General methods for monitoring convergence of iterative simulations. *Journal of Computational and Graphical Statistics*, *7*(4), 434–455. https://doi.org/10.2307/1390675

Cornwell, W. K., Cornelissen, J. H. C., Allison, S. D., Bauhus, J., Eggleton, P., Preston, C. M., … Zanne, A. E. (2009). Plant traits and wood fates across the globe: Rotted, burned, or consumed? *Global Change Biology*, *15*(10), 2431–2449. https://doi.org/10.1111/j.1365-2486.2009.01916.x

Edburg, S. L., Hicke, J. A., Brooks, P. D., Pendall, E. G., Ewers, B. E., Norton, U., … Meddens, A. J. H. (2012). Cascading impacts of bark beetle-caused tree mortality on coupled biogeophysical and biogeochemical processes. *Frontiers in Ecology and the Environment*, *10*(8), 416–424. https://doi.org/10.1890/110173

Feng, Y., & Li, X. (2001). An analytical model of soil organic carbon dynamics based on a simple "hockey stick" function. *Soil Science*, *166*(7), 431–440. https://doi.org/10.1097/00010694-200107000-00001

Fravolini, G., Egli, M., Derungs, C., Cherubini, P., Ascher-Jenull, J., Gómez-Brandón, M., … Marchetti, M. (2016). Soil attributes and microclimate are important drivers of initial deadwood decay in sub-alpine Norway spruce forests. *Science of the Total Environment*, *569-570*, 1064–1076. https://doi.org/10.1016/j.scitotenv.2016.06.167

Freschet, G. T., Weedon, J. T., Aerts, R., van Hal, J. R., & Cornelissen, J. H. C. (2012). Interspecific differences in wood decay rates: Insights from a new short-term method to study long-term wood decomposition. *Journal of Ecology*, *100*(1), 161–170. https://doi.org/10.1111/j.1365-2745.2011.01896.x

Fukami, T., Dickie, I. A., Paula Wilkie, J., Paulus, B. C., Park, D., Roberts, A., … Allen, R. B. (2010). Assembly history dictates ecosystem functioning: Evidence from wood decomposer communities. *Ecology Letters*, *13*(6), 675–684. https://doi.org/10.1111/j.1461-0248.2010.01465.x

García-Palacios, P., Shaw, E. A., Wall, D. H., & Hättenschwiler, S. (2016). Temporal dynamics of biotic and abiotic drivers of litter decomposition. *Ecology Letters*, *19*(5), 554–563. https://doi.org/10.1111/ele.12590

Gora, E. M., Sayer, E. J., Turner, B. L., & Tanner, E. V. J. (2018). Decomposition of coarse woody debris in a long-term litter manipulation experiment: A focus on nutrient availability. *Functional Ecology*, *32*(4), 1128–1138. https://doi.org/10.1111/1365-2435.13047

Harmon, M. E., Fasth, B., Woodall, C. W., & Sexton, J. (2013). Carbon concentration of standing and downed woody detritus: Effects of tree taxa, decay class, position, and tissue type. *Forest Ecology and Management*, *291*, 259–267. https://doi.org/10.1016/j.foreco.2012.11.046

Harmon, M., Franklin, J., Swanson, F., Sollins, P., Gregory, S., Lattin, J., … Cummins, K. (1986). Ecology of coarse woody debris in temperate ecosystems. *Advances in Ecological Research*, *15*, 133–302.

Harmon, M. E., Woodall, C. W., Fasth, B., & Sexton, J. (2008). Woody detritus density and density reduction factors for tree species in the united states: A synthesis. In *General technical report NRS-29* (p. 83). Newton Square, PA: US Dept. of Agriculture, Forest Service, Northern Research Station.

Hérault, B., Beauchêne, J., Muller, F., Wagner, F., Baraloto, C., Blanc, L., & Martin, J. M. (2010). Modeling decay rates of dead wood in a neotropical forest. *Oecologia*, *164*(1), 243–251. https://doi.org/10.1007/s00442-010-1602-8

Hu, Z., Michaletz, S. T., Johnson, D. J., McDowell, N. G., Huang, Z., Zhou, X., & Xu, C. (2018). Traits drive global wood decomposition rates more than climate. *Global Change Biology*, *24*(11), 5259–5269. https://doi.org/10.1111/gcb.14357

Kahl, T., Arnstadt, T., Baber, K., Bässler, C., Bauhus, J., Borken, W., … Gossner, M. M. (2017). Wood decay rates of 13 temperate tree species in relation to wood properties, enzyme activities and organismic diversities. *Forest Ecology and Management*, *391*, 86–95. https://doi.org/10.1016/j.foreco.2017.02.012

Moore, D. J. P., Trahan, N. A., Wilkes, P., Quaife, T., Stephens, B. B., Elder, K., … Monson, R. K. (2013). Persistent reduced ecosystem respiration after insect disturbance in high elevation forests. *Ecology Letters*, *16*(6), 731–737. https://doi.org/10.1111/ele.12097

Moore, T. R., Trofymow, J. A., Prescott, C. E., & Titus, B. D. (2017). Can short-term litter-bag measurements predict long-term decomposition in northern forests? *Plant and Soil*, *416*(1-2), 419–426. https://doi.org/10.1007/s11104-017-3228-7

Mori, S., Itoh, A., Nanami, S., Tan, S., Chong, L., & Yamakura, T. (2014). Effect of wood density and water permeability on wood decomposition rates of 32 Bornean rainforest trees. *Journal of Plant Ecology*, *7*(4), 356–363. https://doi.org/10.1093/jpe/rtt041

O'Hara, R. B., & Sillanpää, M. J. (2009). A review of bayesian variable selection methods: What, how and which. *Bayesian Analysis*, *4*(1), 85–117. https://doi.org/10.1214/09-BA403

Oberle, B., Dunham, K., Milo, A. M., Walton, M., Young, D. F., & Zanne, A. E. (2014). Progressive, idiosyncratic changes in wood hardness during decay: Implications for dead wood inventory and cycling. *Forest Ecology and Management*, *323*, 1–9. https://doi.org/10.1016/j.foreco.2014.03.026

Oberle, B., Milo, A. M., Myers, J. A., Walton, M. L., Young, D. F., & Zanne, A. E. (2015). Direct estimates of downslope deadwood movement over 30 years in a temperature forest illustrate impacts of treefall on forest ecosystem dynamics. *Canadian Journal of Forest Research*, *46*(3), 351–361. https://doi.org/10.1139/cjfr-2015-0348

Oberle, B., Ogle, K., Zanne, A. E., & Woodall, C. W. (2018). When a tree falls: Controls on wood decay predict standing dead tree fall and new risks in changing forests. *PLoS ONE*, *13*(5), https://doi.org/10.1371/journal.pone.0196712

Oberle, B., Ogle, K., Zuluaga, J. C. P., Sweeney, J., & Zanne, A. E. (2016). A Bayesian model for xylem vessel length accommodates subsampling and reveals skewed distributions in species that dominate seasonal habitats. *Journal of Plant Hydraulics*, *3*, 3. https://doi.org/10.20870/jph.2016.e003

Osazuwa-Peters, O. L., Wright, S. J., & Zanne, A. E. (2017). Linking wood traits to vital rates in tropical rainforest trees: Insights from comparing sapling and adult wood. *American Journal of Botany*, *104*(10), 1464–1473. https://doi.org/10.3732/ajb.1700242

Pan, Y., Birdsey, R. A., Fang, J., Houghton, R., Kauppi, P. E., Kurz, W. A., … Hayes, D. (2011). A large and persistent carbon sink in the world's forests. *Science*, *333*(6045), 988–993. https://doi.org/10.1126/science.1201609

Pietsch, K. A., Ogle, K., Cornelissen, J. H. C., Cornwell, W. K., Bönisch, G., Craine, J. M., … Wirth, C. (2014). Global relationship of wood and leaf litter decomposability: The role of functional traits within and across plant organs. *Global Ecology and Biogeography*, *23*(9), 1046–1057. https://doi.org/10.1111/geb.12172

Piñeiro, G., Perelman, S., Guerschman, J. P., & Paruelo, J. M. (2008). How to evaluate models: Observed vs. predicted or predicted vs.

observed? *Ecological Modelling*, *216*(3-4), 316–322. https://doi.org/10.1016/j.ecolmodel.2008.05.006

Plummer, M. (2016). rjags: Bayesian graphical models using MCMC. R package version4-6. Retrieved from https://doi.org/http://cran.r-project.org/package=rjags

R Core Team. (2017). R: A language and environment for statistical computing. Retrieved from http://www.R-project.org/

Ripley, B., Venables, B., Bates, D. M., Hornik, K., & Firth, D. (2015). Support functions and datasets for venables and Ripley's MASS. *R Package*, *"MASS" Version 7.2-45*. ISBN 0-387-95457-0

Spasojevic, M. J., Turner, B. L., & Myers, J. A. (2016). When does intraspecific trait variation contribute to functional beta-diversity? *Journal of Ecology*, *104*(2), 487–496. https://doi.org/10.1111/1365-2745.12518

Spasojevic, M. J., Yablon, E. A., Oberle, B., & Myers, J. A. (2014). Ontogenetic trait variation influences tree community assembly across environmental gradients. *Ecosphere*, *5*(10), https://doi.org/10.1890/ES14-000159.1

Spiegelhalter, D. J., Best, N. G., Carlin, B. P., & Van Der Linde, A. (2002). Bayesian measures of model complexity and fit. *Journal of the Royal Statistical Society. Series B: Statistical Methodology*, *64*(4), 583–639. https://doi.org/10.1111/1467-9868.00353

Van Der Wal, A., Ottosson, E., & De Boer, W. (2015). Neglected role of fungal community composition in explaining variation in wood decay rates. *Ecology*, *96*(1), 124–133. https://doi.org/10.1890/14-0242.1

Venugopal, P., Junninen, K., Edman, M., & Kouki, J. (2017). Assemblage composition of fungal wood-decay species has a major influence on how climate and wood quality modify decomposition. *FEMS Microbiology Ecology*, *93*(3). https://doi.org/10.1093/femsec/fix002

Weedon, J. T., Cornwell, K., Johannes, H. C., Zanne, A. E., Wirth, C., & Coomes, D. A. (2009). Global meta-analysis of wood decomposition rates : A role for trait variation among tree species? *Ecology Letters*, *12*, 45–56. https://doi.org/10.1111/j.1461-0248.2008.01259.x

Witkamp, M. (1966). Decomposition of Leaf Litter in Relation to Environment, Microflora, and Microbial Respiration. *Ecology*, *47*(2), 194–201. https://doi.org/10.2307/1933765

Zanne, A. E., Oberle, B., Dunham, K. M., Milo, A. M., Walton, M. L., & Young, D. F. (2015). A deteriorating state of affairs: How endogenous and exogenous factors determine plant decay rates. *Journal of Ecology*, *103*(6), 1421–1431. https://doi.org/10.1111/1365-2745.12474

Zimmerman, J. K., Pulliam, W. M., Lodge, D. J., Quiñones-Orfila, V., Fetcher, N., Guzmán-Grajales, S., … Guzman-Grajales, S. (1995). Nitrogen immobilization by decomposing woody debris and the recovery of tropical wet forest from hurricane damage. *Oikos*, *72*(3), 314. https://doi.org/10.2307/3546116

SUPPORTING INFORMATION

Additional supporting information may be found online in the Supporting Information section.

How to cite this article: Oberle B, Lee MR, Myers JA, et al. Accurate forest projections require long-term wood decay experiments because plant trait effects change through time. *Glob Change Biol*. 2020;26:864–875. https://doi.org/10.1111/gcb.14873